3.3.3 LTSK9

Vegetation Index

A. Algorithm Outline

(1) Algorithm Code: LTSK9

(2) Product Code: VGI

(3) PI names: G18 Dr. Alfredo Huete

(4) Overview of algorithm (Standard level)

Algorithm objectives

The algorithms has the following objective :

- To compute two vegetation indices (VI's) from the atmospherically corrected and composited reflectances;
  - The normalized difference vegetation index (NDVI) and
  - The enhanced vegetation index (EVI).
- To produce global vegetation index maps on a consistent temporal (16 days) and spatial (1km) resolution

B. Theoretical Description

(1) Methodology and Logic Flow

A general flowchart describing the vegetation index algorithm is presented in figure 1. The vegetation index algorithm will process atmospherically corrected data generated by LTSK 1. Both normalized difference vegetation index (NDVI) and the enhanced vegetation index (EVI) maps will be produced for this phase.

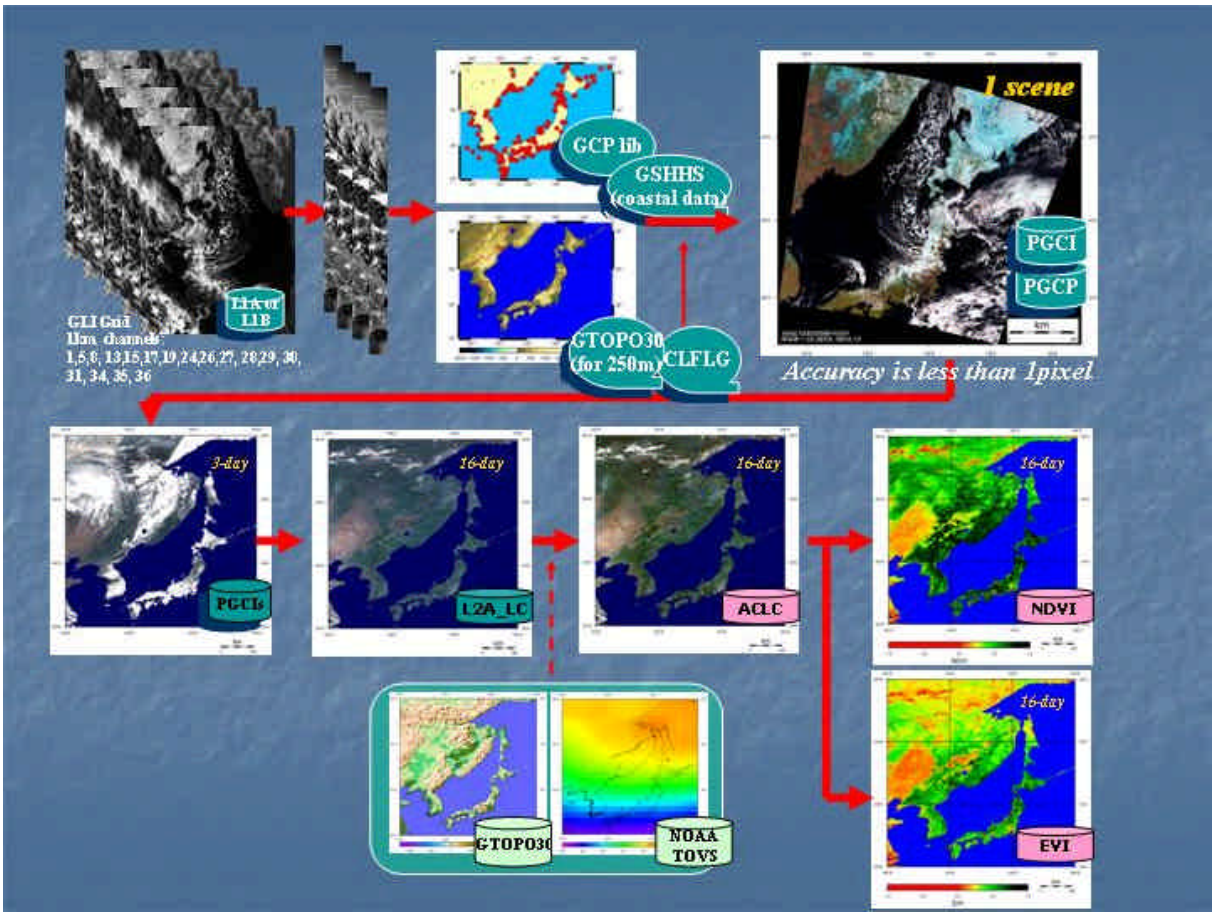

Figure 1: Flow diagram for Vegetation Index (LTSK 9).

(2) Physical and Mathematical Aspects of the Algorithms

GLI vegetation index products

Operational monitoring of the earth's vegetative cover currently involves the utilization of spectral vegetation indices (VI's) as precise radiometric measures of spatial and temporal patterns of vegetation photosynthetic activity, vegetation condition, and vegetation change. VI's are designed to measure spatial and temporal changes in vegetation at regional, continental, and global scales on an inter-annual and seasonal basis. They are also used as intermediaries in the assessment of various plant biophysical parameters, such as leaf area index (LAI), percent green cover, green biomass, and fractional absorbed photosynthetically active radiation (fAPAR). Since their role is to measure 'variations' or changes in vegetation, they are not restricted to the measurement of a single parameter, such as LAI. Vegetation indices are thus highly useful in the detection of any type of vegetation change, regardless of type of change, whether it is a change in biophysical parameter, species composition, stress, land-use, or a combination of change factors.

The compositing approach developed here allows for the computation of numerous vegetation indices, in that it is the reflectances that are composited in a consistent fashion. The computation of the vegetation index then becomes straightforward and unlike other approaches, one can compute and implement different VI's at local, regional, or global scales. Two different VI's are proposed for the GLI instrument; one is a standard, normalized difference vegetation index (NDVI) and the other is an enhanced vegetation index (EVI). The NDVI, which is the ratio between the difference in the red and near-infrared and their sum, has been the most widely used index in global vegetation studies, including phenological studies of vegetation growing season; land cover classification; and global climate system models (Goward et al. 1985; Townshend et al. 1994; Tucker and Seller 1986; Malingreau et al. 1989; Justice et al. 1985; Sellers et al. 1994; Townshend et al. 1991). These studies have shown a qualitative correspondence of differences in NDVI with observed or recognized variations in vegetation growth. With appropriate 'translation coefficients', the NDVI global data set acts as a continuity index allowing one to take advantage of a 25 year AVHRR-NDVI data record as well as to couple a GLI-NDVI with a MODIS-NDVI, etc. The translation coefficients involve simultaneous measurements of NDVI over validation test sites and take into account differences

in sensor bandwidths, center wavelengths, and calibration accuracies.

The NDVI is a scaled, non-linear transform of the simple ratio (SR = NIR/red), originally developed to enhance the vegetation signals over sparsely vegetated rangelands (Deering, 1978);

$$NDVI = (\rho_{nir} - \rho_{red}) / (\rho_{nir} + \rho_{red}). \quad (1)$$

The NDVI retains certain favorable ratioing properties, which reduce noise and uncertainty associated with instrument characteristics and external sources of noise (e.g., cloud shadows). There are also certain disadvantages, including non-linearity and scaling problems; an asymptotic (saturated) signal at the high biomass end of vegetated canopies (figure 2), and sensitivity to canopy backgrounds (soil, litter, snow…) over open canopy conditions (Huete et al., 1997).

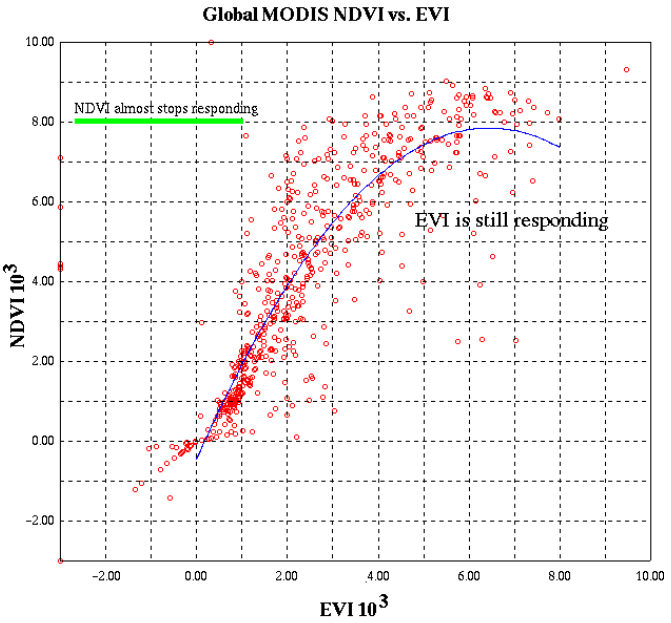

Figure 2: NDVI saturation.

Progress toward improved monitoring of vegetation patterns and biospheric processes is partly restricted by limitations of the sensor systems and partly by inherent limitations of using empirical or semi-empirical spectral indices (Goward et al. 1991; Myneni et al. 1995). Goward et al. (1991) state that errors of ±50% are possible with the AVHRR-NDVI product owing to such factors as poor sensor calibration, poor image registration, variable angular-induced pixel sizes, and incomplete cloud screening.

We also propose the use of a new 'enhanced vegetation index' (EVI) for increased sensitivity over a wider range of vegetation conditions, removal of soil background influences, and removal of residual atmospheric contamination effects present in the NDVI. The soil background adjustment is based on the soil adjusted vegetation index (SAVI) (Huete 1988; Huete et al. 1994); which optimizes the NDVI by accounting for differential red and near-infrared extinction through a photosynthetically active canopy via Beer's law (Fig. 3);

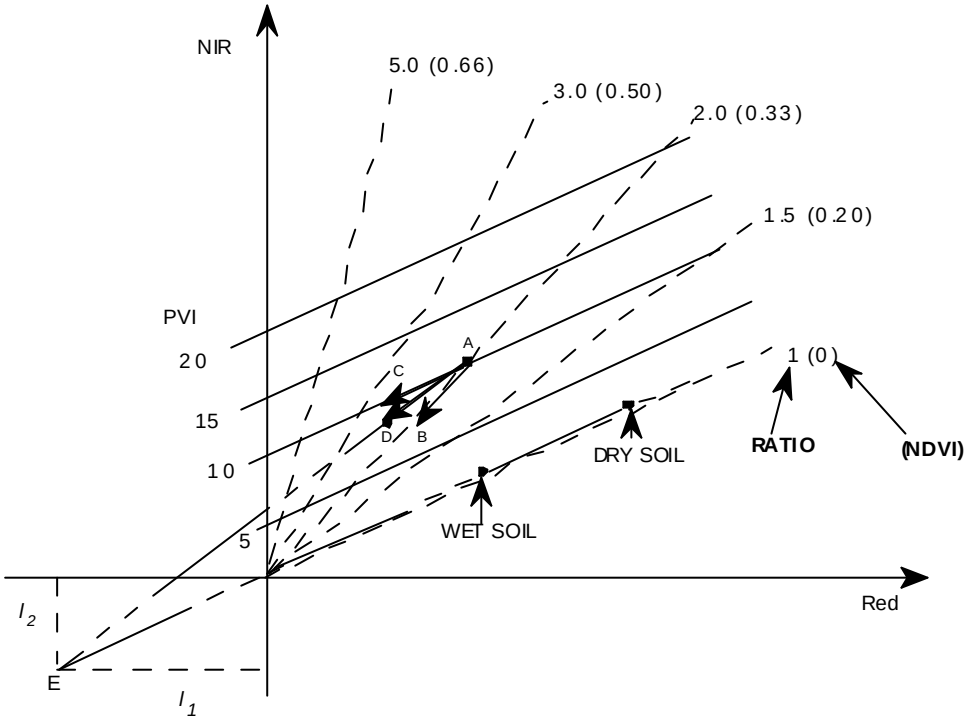

Figure 3. Optimization of the NDVI for canopy background correction via use of vegetation isolines in accordance with Beer's law.

An atmospheric resistant term, derived from the atmospherically resistant vegetation index (ARVI) (Kaufman and Tanré 1992) is included to correct for variable aerosol effects in the red band on a pixel by pixel basis. The ARVI utilizes the difference in radiance between the blue and red channels, via a γ function, to correct the radiance in the red channels and stabilize the index to temporal and spatial variations in gaseous and particulate pollutants. The enhanced vegetation index (EVI) was developed to optimize the vegetation signal from deserts to rainforests while minimizing aerosols and canopy background sources of uncertainty (Liu and

Huete, 1995). The feedback-based structure of the equation takes the form:

$$EVI = 2.5\ (\rho_{nir} - \rho_{red}) / (L + \rho_{nir} + C_1\ \rho_{red} - C_2 \rho_{blue}), \quad (2)$$

where L is the canopy background and snow correction caused by differential NIR and red radiant transfer (transmittance) through a canopy; and C1 and C2 are the coefficients of the aerosol 'resistance' term, which uses the blue band to correct for aerosol effects in the red band (Kaufman and Tanre, 1992). This equation is not as effective as the NDVI in 'ratioing' bands to remove noise, and thus is susceptible to the noise and uncertainty remaining in instrument calibration and in the derivation of atmospherically-corrected reflectances. However, aerosol variations are considerably reduced via the self-correcting combination of the red and blue channels and today's sensors, such as GLI, as less prone to instrument noise compared with the AVHRR. The currently used coefficients, L = 1; C1 = 6; and C2 = 7.5, are fairly robust and have been applied to Landsat TM, ground observation data, and simulated canopy model data (Liu and Huete, 1995, Huete et al 1997).

Huete et al. (1996) found that the EVI can refine global vegetation studies by extending the range of sensitivity of the VIs into both

- Densely vegetated, forested regions, and
- Sparsely vegetated, arid and semi-arid regions.

Figure 4 shows the performance of both NDVI and EVI over a wide range of conditions including:

- Vegetation temporal dynamics
- Atmosphere condition (clouds and aerosol)
- Varying viewing geometry

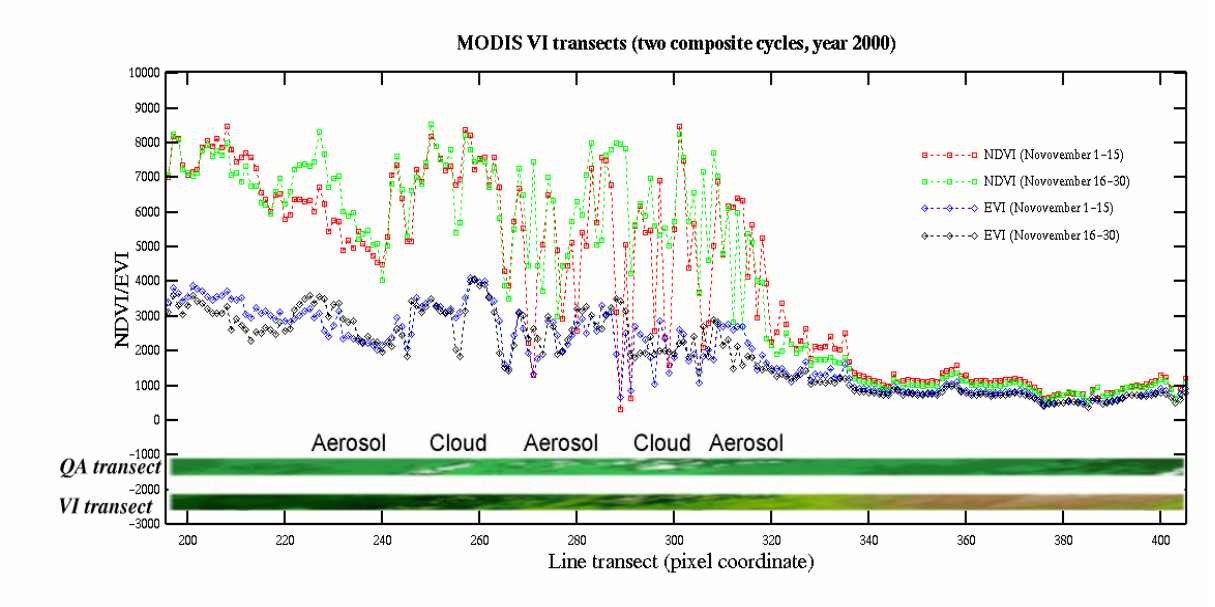

Figure 4: VI performance over variable atmosphere conditions, viewing geometry, and vegetation. The stability of EVI is due in part to its atmosphere resistance

Increased sensitivity in densely vegetated areas was accomplished by placing more weight to the NIR reflectance component of the EVI equation. The less absorbing and greater penetration and scattering properties of the NIR enables increased sensitivity to green biomass and prevents VI saturation at the highest levels of vegetation (Figure 5). In this figure we see the saturation of the NDVI over densely vegetated, forested areas depicted in the form of histograms, where the NDVI has clearly saturated while the EVI maintains a normal distribution which better represents the large range in LAI values in this scene (LAI = 2 - 8).

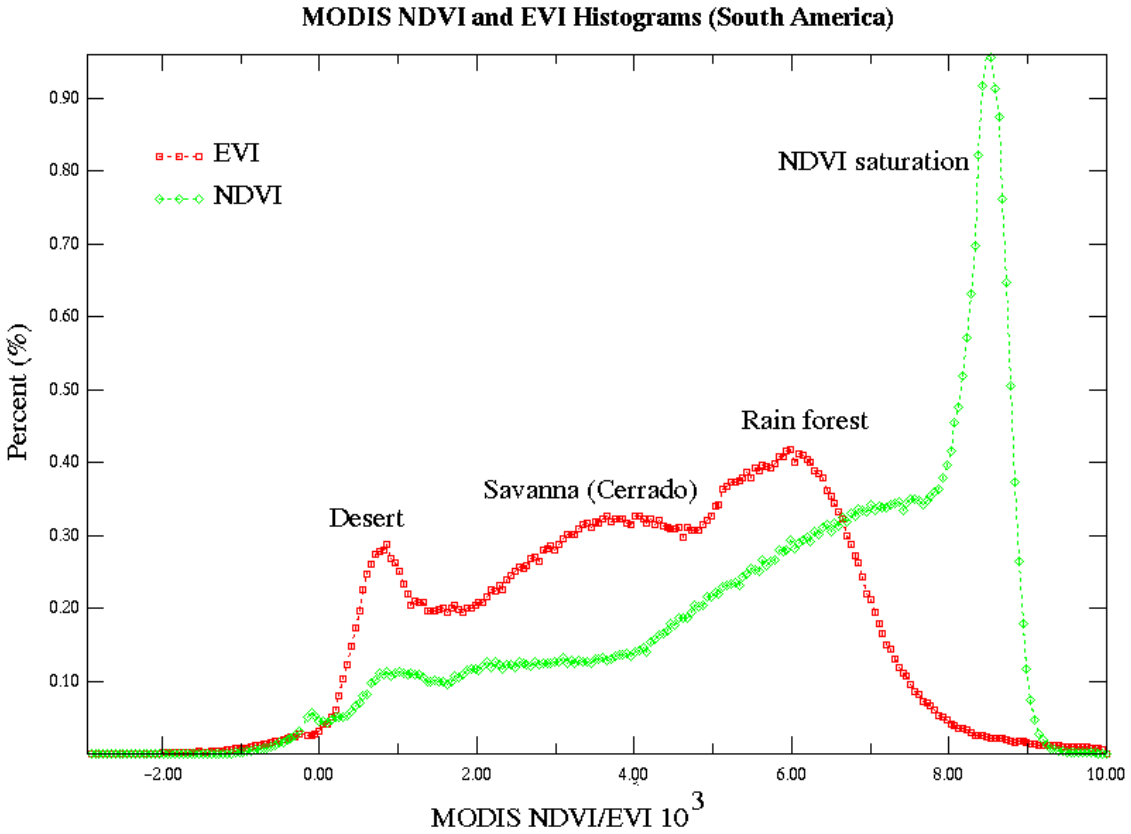

Figure 5. NDVI and EVI histograms of a MODIS scene over South America

Changes in land use, land cover, and net primary production are difficult to detect in a 'saturated' mode (Townshend et al. 1991, Huete et al, 1997). An index, such as EVI with extended, linear response over a wider range of vegetation conditions would not only minimize the 'saturation' problem but would also allow for more accurate aggregation and scaling of multi-resolution data sets. In Fig. 6, an example of the difficulty in detection of land use changes with a 'saturated' NDVI is shown relative to the SAVI and EVI.

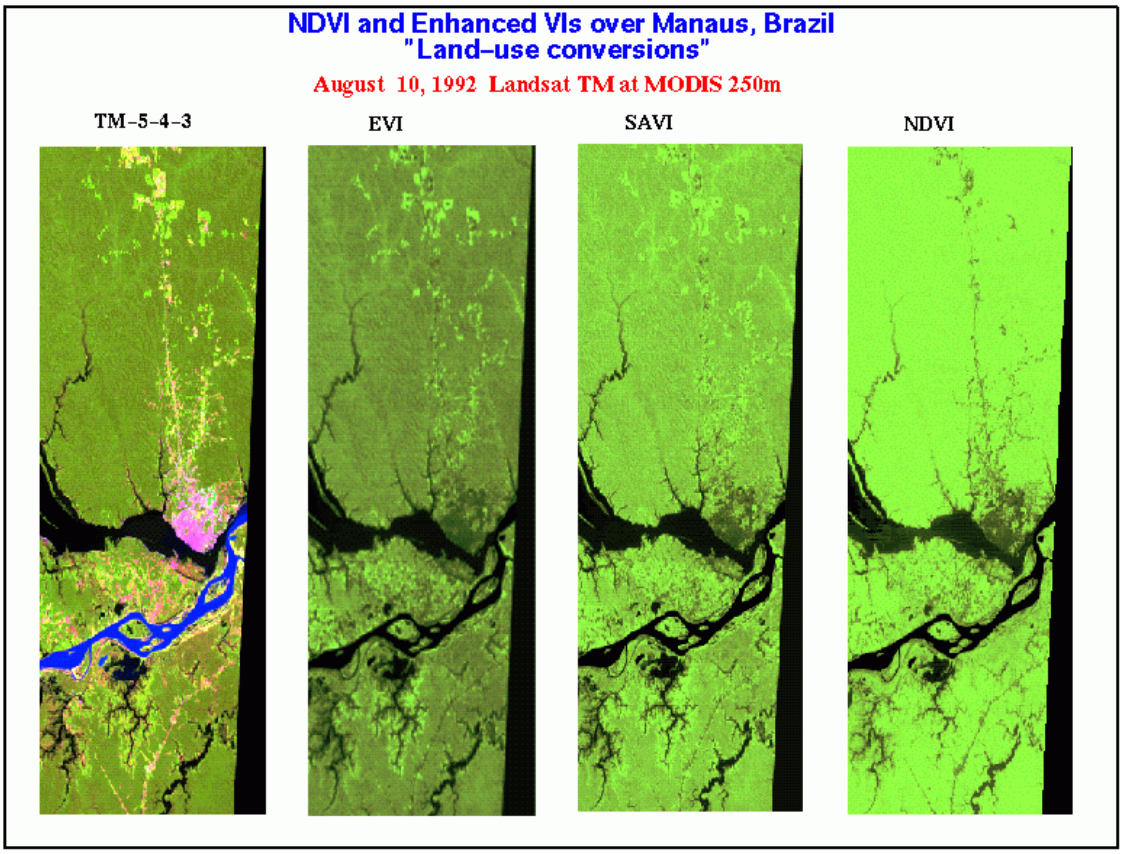

Figure 6. 250 m simulated imagery from Landsat TM over Amazon Forest showing land use clearing in the top portion of the image.

The aerosol correcting methodology is shown below for the EVI (Fig. 7):

(a) Color composite of smoke plume in Oregon TM image.

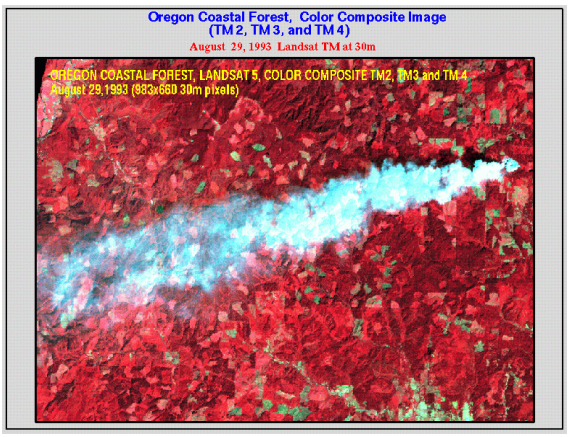

(b) NDVI image of Oregon smoke plume.

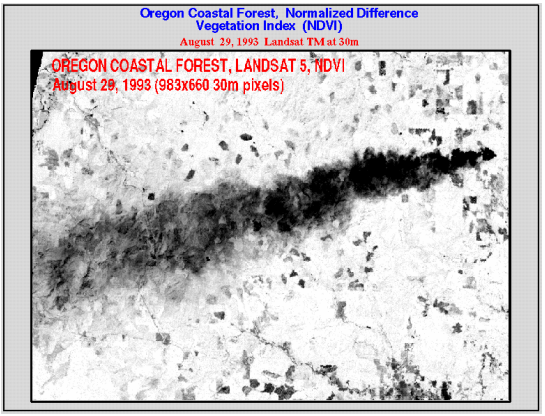

(c) EVI image of Oregon smoke plume.

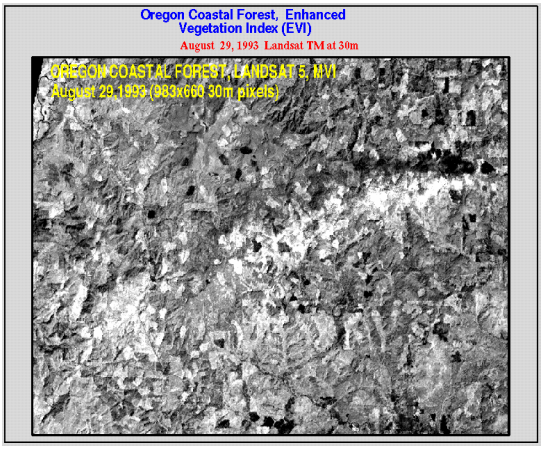

Figure 7. NDVI and EVI images of a smoke plume in Oregon showing aerosol correcting ability of the EVI.

The GLI VI products will be spatially and temporally re-sampled, and designed to provide cloud free vegetation index maps at nominal resolutions of 1 km. The composited surface reflectance data from each pixel is used to compute both the NDVI and the EVI gridded products. The bands used to compute the VI are as follows:

Red band	GLI band 13	(673-683 nm, 1km band)
NIR band	GLI band 19	(860-870 nm, 1km band)
Blue band	GLI band 5	(450-470 nm, 1km band)

These bands are much narrower than the 250m equivalent bands, and provide increased chlorophyll sensitivity (band 13) and avoids water vapor absorption (band 19). The blue band provides aerosol resistance in the EVI.
The gridded VIs is produced at 16-day (half-month). Monthly gridded VI products will also be produced but based on temporal averaging of the 16 days products.

C. Practical Considerations

In this section we shall explore some of the proposed algorithms aspects with respect to implementation, programming and data interfacing.

(1) Programming, Procedural, Running Considerations

1.1 Compositing and Vegetation Index Algorithm Implementation

Due to the flow of data within the land processing algorithms (figure 1), the compositing algorithm (LTSK 10) executes first and generates one data set representative of the composite period (16 days). The atmosphere correction algorithm (LTSK 1) follows and generates the atmospherically corrected surface reflectance product for Rayleigh and Ozone. Once this corrected surface reflectance data is present (L2A_LC) the vegetation index algorithm (LTSK 9) executes and generates the same data set with the addition of vegetation indices (NDVI, EVI). This algorithm is simple, in that most of the work was performed earlier by LTSK 10, and LTSK 1. Hence, it only computes both NDVI and EVI and appends them to the L2A_LC standard product.

Figures 8 to 12 are 16 day prototype product of the global GLI-NDVI/EVI , they are the result of applying the GLI-MVC/CMVC algorithm to a set of SeaWiFS and MODIS daily global data. We note that the SeaWiFS data is corrected for Rayleigh and ozone absorption and has a resolution of 8x8 km, covering the entire globe, MODIS on the other hand is corrected for all atmospheric contaminations including aerosol. These prototyping exercises show favorable results and indicate that the algorithm is performing very well and as designed.

1.2 Numerical and computation considerations

As described above, the LTSK 9 algorithm is a continuation of the LTSK 10 algorithm. Atmospherically corrected reflectance resulting from the LTSK 1 algorithm are simply used to compute NDVI and EVI. The LTSK 9 algorithm will process each L2A_LC scene and the resulting product archived. This algorithm will run once every 16 days on the GLI gridded data sets. Computationally this algorithm is not demanding because LTSK 10 carried the most crucial work of compositing the data earlier and the LTSK 1 performed the atmosphere correction.

(2) Calibration and Validation

2.1 GLI VI prototyping with SeaWiFS data

A month's worth of daily SeaWiFS data (September 1997)were obtained from the GSFC (Nazmi Saleous, 1998) to test and prototype the GLI vegetation index compositing algorithm. The daily data was mapped to a global 8 km equal area grid, resulting in global spatial dimensions of 2500 by 5000 pixels (Rows and Columns). The SeaWiFS data was in the Hierarchical Data Format (HDF) and consisted of 11 data fields (Reflectances, Geolocations). It is important to mention that GLI consists of 9 land bands (1km band) and in the processes to generalize our algorithm we copied the 8th SeaWiFS band to create the 9th GLI band. The reflectance data was corrected for Rayleigh scattering and ozone absorption. Cloud flags were produced during the execution by using a maximum BLUE band of 0.25 (Any data above the 0.25 mark is considered cloudy). The land/sea mask was an ancillary data layer acquired with the global data sat. More specific information on the SeaWiFS data can be found on the NASA internet home page.

Daily, global 8 km SeaWiFS data were processed to prototype the GLI-MVC and GLI-constrained view angle MVC (CMVC) vegetation index compositing algorithms. Both NDVI

and EVI were produced. Figures 8 - 11 depict the results of this prototyping technique.We note also that the current algorithm has built in flexibility to assess the differences between MVC and CMVC, in conjunction with the cloud cover.

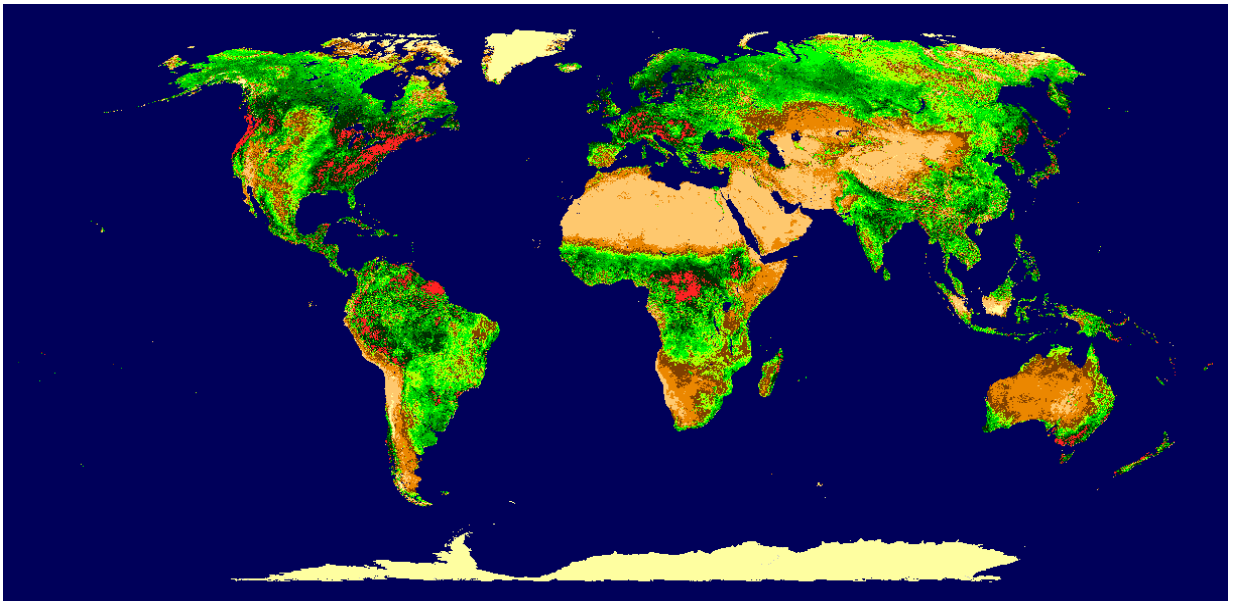

Figure 8. NDVI composite: GLI MVC algorithm prototype with SeaWiFS data set.

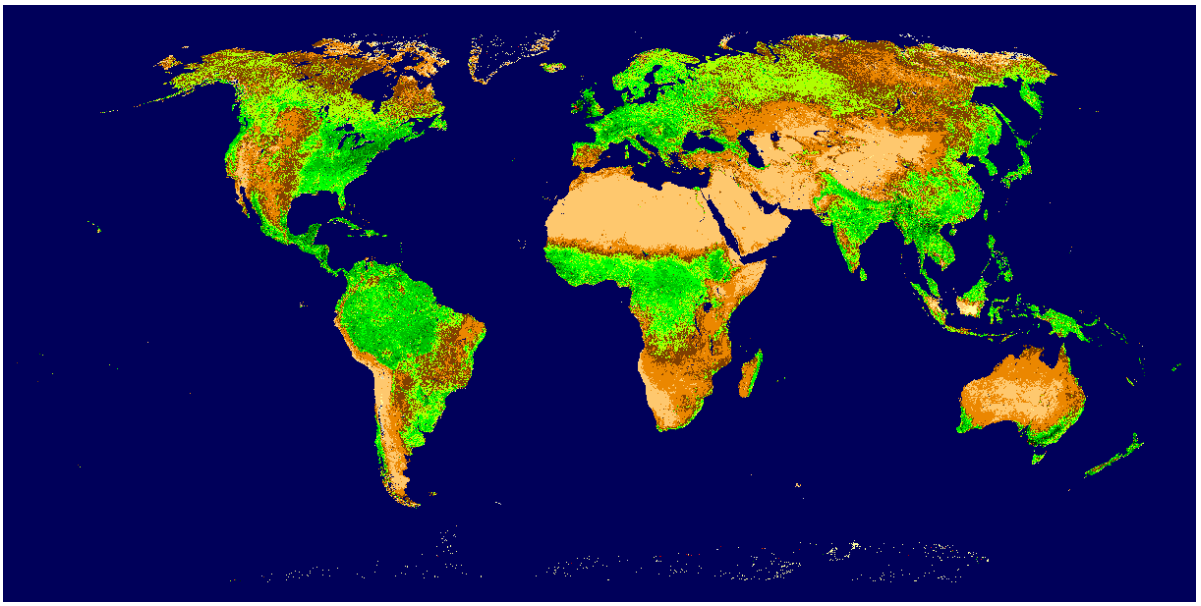

Figure 9. EVI composite: GLI MVC algorithm prototype with SeaWiFS data set.

2.2 GLI VI prototyping with MODIS data

We extensively used MODIS data (available since April 2000) to prototype the GLI vegetation index and compositing algorithms. Due to the science similarity of the MODIS and GLI compositing algorithms, the results of this prototyping were very comparable (figure 12-15).

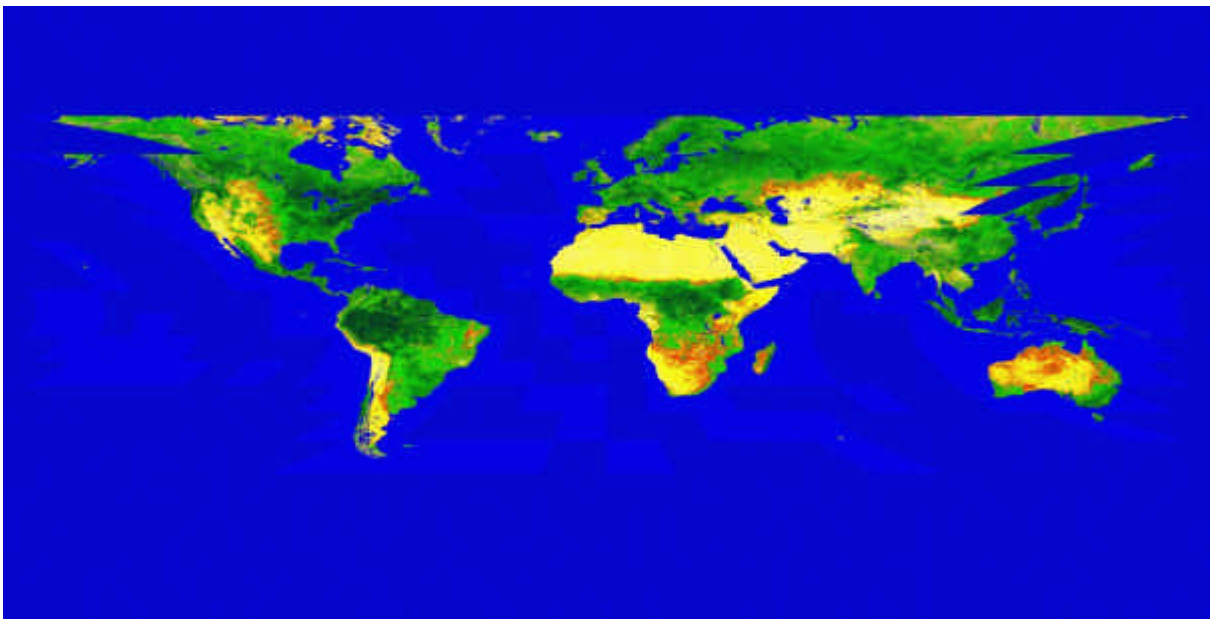

Figure 10: GLI NDVI, CV-MVC prototype using MODIS data. (Equal-rectangular projection)

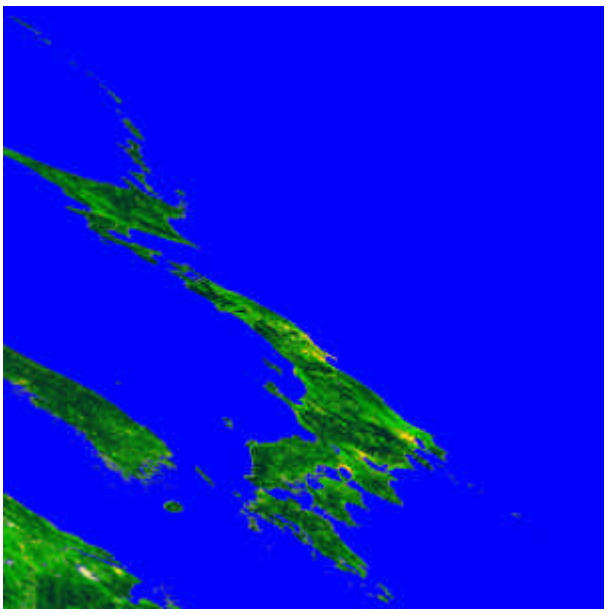

Figure 11: GLI NDVI map of the Japanese islands (prototype with MODIS data)

2.3. Validation of the GLI Vegetation Index product

There are two 'distinct' VIs, designed to measure different properties of the vegetation canopy. There is the NDVI, which is very useful in deriving two-dimensional vegetation parameters such as fAPAR and percent green cover; and there is the enhanced vegetation index (EVI), which is strongly correlated with canopy structural parameters, such as leaf area index (LAI). These two VIs are unique in that the NDVI will quickly 'saturate' under high biomass conditions (as does %cover and fAPAR) of agriculture and forests. The EVI does not saturate and maintains sensitivity throughout the Earth's biomes, including tropical rainforests. Because the EVI is sensitive to structural parameters, it is easy to detect land use changes/conversions as well, as in the Amazon deforestation (the NDVI is useless and saturates out). Furthermore, the EVI is not sensitive to canopy background and can be designed to remove (minimize) aerosol influences. This is important since GLI will not have aerosol corrections over land (only oceans).

We have used 'real' ground radiometric data over various crops and grasses, including corn, cotton, sorghum, and wheat. We have also created a Landsat TM-based global biome data set and have tested/developed our algorithms over all biome types such as desert, grasslands, woodlands, forests, etc..., with snow conditions, lakes, and burning (smoke) conditions. Finally, we are using the SAIL and DISORD (Myneni) canopy radiant transfer models to verify and understand the nature of the algorithms.

There are two components to the validation of the VI:

(2) First there is a radiometric validation since the VIs are unitless and dependent on the quality of the input (reflectance) parameters;

(3) secondly, there is the biophysical validation of the VIs or the outputs of the VI equation - to see that the VI really measures a change in vegetation amount and that sensitivity is maintained throughout the wide range of environmental conditions on the planet.

For the radiometric part, we are using field radiometers that can be flown on light aircraft (or helicopter) just above the canopies. These need not be expensive and can be non-imaging spectral profilers (radiometers). We also need the radiometer to measure background reflectance properties, understory and soil, and canopy transmittance (in forests). For the biophysical part,

we plan to implement LAI and fAPAR sensors, like ceptometers, quantum sensors, and LAI LiCOR-2000 instruments.

2.3.1 Validation procedure:

In the radiometric sense, we will validate by ensuring that the top-of-canopy reflectances/ VI's agree with that from the GLI sensor. The top-of-canopy values encompass the average of airborne, linear transects of at least 1 km length. The 1 km transects encompass a homogeneous patch of the dominant land cover type. Additional transects are flown beyond the homogeneous site to cover the natural heterogeneity of any given 10 km by 10km area, including 'endmembers'. The measurements are made (helicopter/aircraft) at below 150 m altitude to avoid atmospheric effects. Nadir values are obtained and matched with those from GLI (adjusted to nadir view pixels). The measurements are made prior to and after the time of GLI overpass to ensure solar zenith angle correspondence. The airborne radiometers are calibrated and extended to GLI sensor responses via simultaneous measurements made at bright and dark, uniform, non-vegetated sites. Sun photometers are needed to characterize and correct for the atmosphere. The figure below shows the Radiometric validation component.

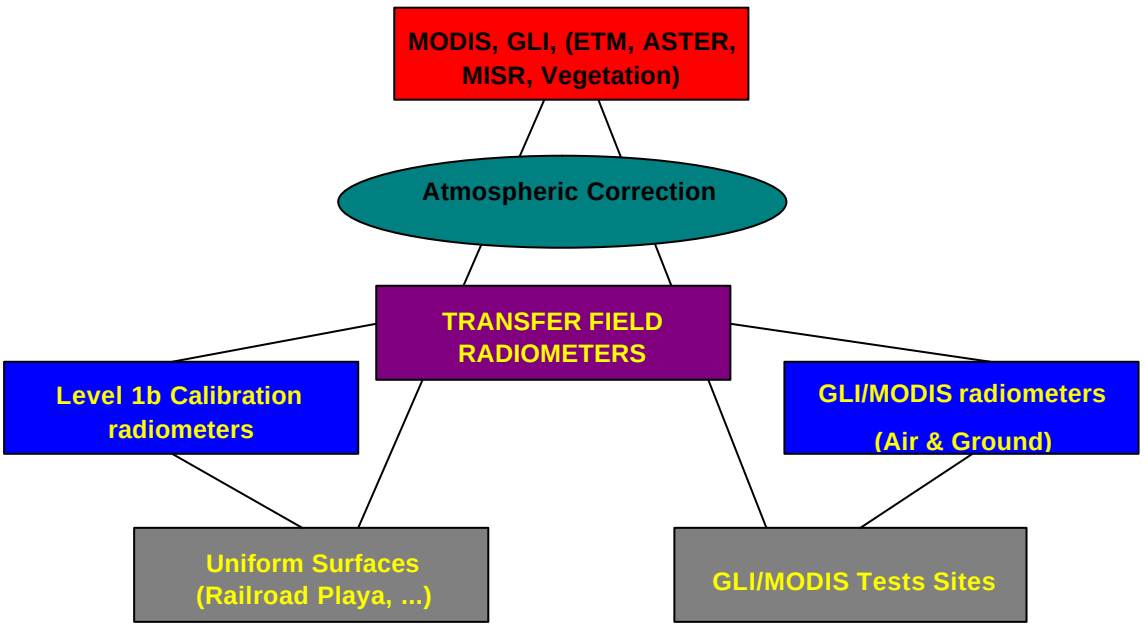

Figure13: Radiometric validation component

In a biophysical sense, 1km transects of biophysical measurements need to be collected on the ground. Percent cover is obtained from digital aerial photos (on the same aircraft/ helicopter with the radiometer). Leaf area index (LAI) is measured through linear transects of 1 km length with LiCOR-LAI 2000. The error and uncertainty of the LAI measurements are to be obtained from smaller subplots involving direct LAI leaf sampling. LAI is also measured outside the homogeneous site at lower and higher LAI conditions, so that a relationship curve between VI and LAI can be plotted for that biome type. All measures are to be taken over a window of standard solar zenith angles.

For the fAPAR measures, ceptometers and quantum sensors are used over a set of limited subplots within the 1 km LAI transects. Measurements of fAPAR are made over a large range of sun angles (entire morning or diurnally), since fAPAR is very sensitive to sun angle and because fAPAR will be used by the NPP product which requires 'daily' fAPAR values.

Biophysical measures need to be made over the following land cover types (biomes), each encompassing a range of low to high vegetation amounts.

- Shrublands (hyper-arid to semi-arid)
- Grasslands (semi-arid to humid)
- Cereal and broadleaf crops (entire growing season)
- Savannas (woodlands) low to dense trees
- Broadleaf Forests (temperate and tropical regions)
- Needleleaf Forests
- Mixed Forests

2.3.2 Validation test sites (preliminary)

At minimum one site is needed per biome type listed above. Ideally two or three sites per biome are desired to ensure enough global variability to develop a global validation and error/ uncertainty analysis. We also need a couple of 'baseline' sites with no vegetation, like Atacama, Gobi, Sahara, etc... These sites are needed to monitor sensor degradation and drift as well as to readily calibrate/match GLI sensor responses with field instrumentation. Validation work is being conducted in cooperation with Japanese validation teams, and in conjunction with the MODIS validation effort.

(3) Quality Control and Diagnostic Information

Applying complex algorithms to remote sensing data will increase its uncertainty, the amount of noise, and possibly create values that are not accurate. The idea of implementing QA/QC checks evolved from previous work with AVHRR. On a pixel basis data will be characterized by its cloudiness, state of the sensor during on board registration, georeferencing problems, performance of the algorithms that generated the data, all of which contribute to the final quality. For instance the computation of the VIs uses spectral responses at different positions, it also involves simple difference and rationing, which can lead to floating point and overflow errors. These types of errors are captured during execution and appended to the data as quality assurance flags that could be used to assess the usefulness of the product and to characterize its validity (figure 14).

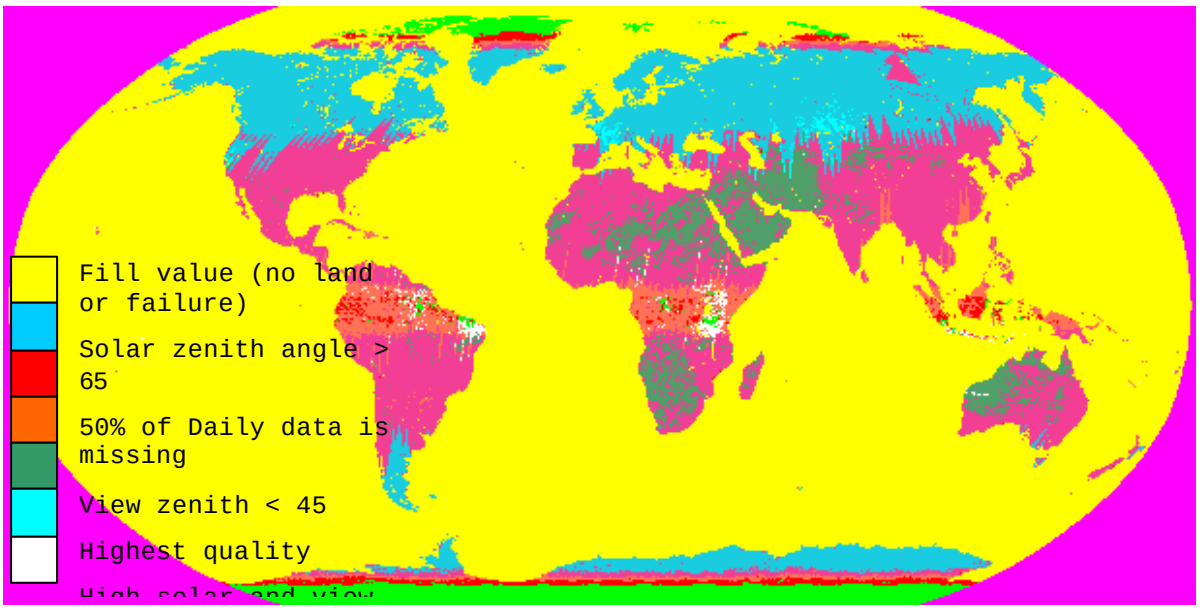

Figure 14: GLI prototype quality layer

(4) Exception Handling

As described in the previous sections, a solid scheme for capturing error and conveying them to the end user is implemented. During execution, all computation errors, out of range data, and missing inputs are passed to the user via pre-defined fill values and quality flags. In case of algorithm failure, the processing code will generate messages that indicates the source and

possible remedies to the errors.

(5) Constraints, Limitations, Assumptions

Although the algorithm was designed and optimized for processing GLI data, some of the assumption in the design were based on other sensor (MODIS, SeaWiFS, and AVHRR). The performance and accuracy of the algorithm have so far been measured using data from both SeaWiFs and MODIS, some of them are:

- GLI bands used for VI computation are much narrower and could exhibit excessive sensitivity
- The vegetation indices are computed based on atmosphere correction performed on composited data, this idea was never tested in operational mode.
- The orbital coverage of GLI (4 observations at the equator) could affect the resulting VI product because of the persistence of clouds in that region. Usually more data is required in these regions to effectively remove clouds.

Overall, we expect the current algorithm to perform very well. All prototyping indicates that EVI is expected to be a robust global vegetation index, owing to its atmosphere resistance (which is crucial in the case of GLI given the lack of aerosol correction) and its increased sensitivity to vegetation variability.

(6) Suggestions and Recommendations

Since data is only corrected for Rayleigh and Ozone and the difference of the bands used, the resulting GLI VI will most likely deviate from those produced by MODIS. It is then important to take this into considerations when performing across sensor comparison of results. Moreover, the compositing scheme is performed prior to atmosphere correction, this will further complicate any translation between sensors. Nonetheless, this GLI processing scheme has its advantages:

- Simpler data processing
- MVC/CV-MVC should perform better on non-atmospherically corrected data
- Continuity with AVHRR is easily established due to the similar atmosphere correction scheme.

We recommend that the validation of the atmospherically corrected surface reflectance product

should be rigorous. This will insure its validity and quality along with that of the GLI VI.

D. References

Ackerman, S., K. Strabala, P. Menzel1, R. Frey, C. Moeller, L. Gumley, B. Baum, C. Schaaf, G. Riggs, R. Welch, 1996. Discriminating Clear-sky from Cloud with Modis Algorithm Theoretical Basis Document V3, http://eospso.gsfc.nasa.gov/atbd/modistables. html.

Agbu, P.A., and James, M.E., 1994. The NOAA/NASA Pathfinder AVHRR Land Data Set User's Manual. Goddard Distributed Active Archive Center, NASA, Goddard Space Flight Center, Greenbelt.

Asano, S. and Uchiyama, A. (1987), Application of an extended ESFT method to calculation of solar heating rates by water vapor absorption, J.Quant. Spectrosc. Radiat. Transfer, 38. 147-158.

Asrar, G., Fuchs, M., Kanemasu, E.T. and Hatfield, J.L., 1984, Estimating absorbed photosynthetic radiation and leaf area index from spectral reflectance in wheat, Agron. J., 76:300—306.

Asrar, G., Myneni, R.B., and Choudhury, B.J., 1992, Spatial heterogeneity in vegetation canopies and remote sensing of absorbed photosynthetically active radiation: a modeling study. Remote Sens. Environ. 41:85-101.

Baret, F., and Guyot, G., 1991. Potentials and limits of vegetation indices for LAI and APAR assessment. Remote Sens. Environ. 35: 161-173.

Bohren, C.F. and Huffman,D.R. (1983), Absorption and Scattering of Light by Small Particles, Wiley-Interscience, New York.

Chandrasekhar, S. (1960), Radiative Transfer, Dover, New York.Coulson, K.L., (1988) Polarization and Intensity of Light in the Atmosphere, A. Deepak, Hampton, Virginia.

Choudhury, B.J., 1987, Relationships between vegetation indices, radiation absorption, and net photosynthesis evaluated by a sensitivity analysis, Remote Sens. Environ. 22:209-233.

Cihlar, J., Manak, D., and D'Iorio, M., 1994b. Evaluation of Compositing Algorithms for AVHRR Data over Land. IEEE Trans. Geosc. Remote Sens., 32:427-437.

Cihlar, J., Manak, D., and Voisin, N., 1994a. AVHRR Bidirectional Reflectance Effects and Compositing. Remote Sens. Environ., 48:77-88

Cihlar, J.C., H. Ly, Z. Li, J. Chen, H. Pokrant, and F. Huang, 1997. Multitemporal, Multichannel AVHRR data sets for Land Biosphere Studies— Artifacts and Corrections. Remote Sens. Environ. 60:35-57.

Deering, D.W. and Eck, T.E., 1987. Atmospheric optical depth effects on angular anisotropy of plant canopy reflectance. Int. J. Remote Sensing, 8(6), 893-916.

Deering, D.W. and Leone, 1986. A sphere-scanning radiometer for rapid directional measurements of sky and ground radiance, Remote Sens. Environ., 19:1-24.

Eidenshink, J.C. and Faundeen, J.L., 1994, "The 1km AVHRR global land data set: first stages in implementation," Int. J. Remote Sensing, 15(17), pp. 3443-3462.

Fung, Y., Tucker, C.J. and Prentice, K.C., 1987. Application of Advanced Very High Resolution Radiometer Vegetation Index to Study Atmosphere-Biosphere Exchange of CO_2. J. Geoph. Res., 92, 2999-3015.

Giver, L.P., Benner, D.C., Tomasko, M.G., Fink, U. and Kerola, D.X.(1990), Gaussian quadrature exponential sum modeling of near infrared methane laboratory spectra obtained at temperatures from 106 to 297 K.,in First International Conference on Laboratory Research for Planetary Atmospheres, pp. 147-156. NASA CP 3077.

Goody, R.M. and Yung, Y.L. (1989), Atmospheric Radiation: Theoretical Basis, Second Edition, Oxford University Press, New York.

Gordon, H.R., Brown, J.W., and Evans, R. H. (1988), Exact Rayleigh scattering calculations for use with the Nimbus-7 Coastal Zone Color Scanner, Applied Optics, **27**, 862-871.

Goward, D.G., Turner, S., Dye, D.G., and Liang, J., 1994. University of Maryland improved Global Vegetation Index. Int. J. Remote Sensing, 15(17), 3365-3395.

Goward, S.N. Dye, D.G., Turner, S., and Yang, J., 1993. Objective assessment of the NOAA global vegetation index data product. Int. J. Remote Sensing, 14, 3365-3394.

Goward, S.N., and Huemmrich, K.F., 1992, Vegetation canopy PAR absorptance and the normalized difference vegetation index: an assessment using the SAIL model, Remote Sens. Environ. 39:119-140.

Goward, S.N., B. Markham, D.G. Dye, W. Dulaney, J. Yang, 1991, "Normalized difference vegetation index measurements from the Advanced Very High Resolution Radiometer", Remote Sens. Environ., 35:257-277.

Gutman, G.G., 1991, Vegetation indices from AVHRR: an update and future prospect, Remote Sens. Environ., 35:121-136._

Hansen, J.E. (1971), Multiple scattering of polarized light in planetary atmospheres. Part II. Sunlight reflected by terrestrial water clouds, J. Atmos. Sci., 28, 1400-1426.

Hansen, J.E. and Travis, L.D. (1974), Light scattering in planetary atmospheres, Space Sci. Rev., 16, 527-610.

Herman, B.M. and Browning, S.R. (1965), A numerical solution to the equation of radiative transfer, J. Atmos. Sci., 22, 559-566.

Holben, B.N. 1986. Characterization of maximum value composites from temporal AVHRR data. Int. J. Remote Sensing, 7:1417-1434.

Huete, A.R. ,1988, A soil adjusted vegetation index (SAVI), Remote Sens. Environ. 25:295-309.

Huete, A.R., Justice, C.O., van Leeuwen, W.J.D., 1996. "MODIS vegetation Index, Algorithm Theoretical Basis Document," http://eospso.gsfc.nasa.gov/atbd/modistables. html.

Huete, A.R., Liu, H.Q., Batchily, K., and van Leeuwen, W., 1997, A comparison of vegetation indices over a global set of TM images for EOS-MODIS, Remote Sens. Environ., 59:440-451.

Iqbal, M. (1983), Introduction to Solar Radiation, Academic Press, New York.

James, M.D., and Kalluri, S.N.V. (1994), The Pathfinder AVHRR land data set: An improved coarse resolution data set for terrestrial monitoring, Int. J. Remote Sensing, 15(17):3347-3363.

Justice, C.O., Townshend, J.R.G., Holben, B.N. and Tucker, C.J.,1985, "Analysis of the phenology of global vegetation using meteorological satellite data", Int. J. Remote Sensing, 6:1271-1318.

Kaufman, Y.J. and Tanré, D., 1992, Atmospherically resistant vegetation index (ARVI) for EOS-MODIS, IEEE Trans. Geosci. Remote Sensing, 30:261-270.

Kerola, D. X. (1994), Near-Infrared Spectroscopic Studies of the Troposphere of Saturn, Ph.D. Dissertation The University of Arizona.

Kerola, D. X. (1996), Polarization and intensity of sunlight in the Earth's atmosphere: revisiting the Gauss-Seidel modeling approach, Bull. Amer. Astron. Soc., 28, 1158.

Kerola, D. X., Larson, H. P ., and Tomasko, M. G. (1997), Analysis of the near-IR spectrum of Saturn: a comprehensive radiative transfer model of its middle and upper troposphere, Icarus, 127, 190-212.

Kimes, D.S., Holben, B.N., Tucker, C.J., and Newcomb, W.W., 1984. Optimal directional view angles for remote-sensing missions. Int. J. Remote Sensing 5(6), 887-908.

Kimes, D.S., Newcomb, N.W., Tucker, C.J., Zonneveld, I.S., Van Wijngaar-den, W. De Leeuw, J. and Epema, G.F.(1985), Directional reflectance factor distributions for cover types of northern Africa, Remote Sens. Environ., 17, 1-19.

Kimes, D.S., Newcomb, W.W., Tucker, C.J., Zonneveld, I.S., Van Wijngaarden, W., De Leeuw, J., and Epema, G.F., 1985. Directional Reflectance Factor Distribution for Cover Types of Northern Africa. Remote Sens. Environ. 18:1-19.

Kuchler, A.W., 1995. Natural vegetation map, In: Rand McNally Goode's World Atlas; 19th edition. Eds. Espenshade E.B. Hudson, J.C., Morrison, J.L.. p 18-19.

Lacis, A. (1990), private communication. Leckner, B. (1978), The spectral distribution of solar radiation at the earth's surface - elements of a model, Solar Energy, 20(2), 143-150.

Leeuwen van, W.J.D. A.R. Huete, S. Jia, C.L Walthall, 1996. Comparison of Vegetation Index Compositing Scenarios: BRDF Versus Maximum VI Approaches. IEEE- IGARSS'96, Lincoln Nebraska, Vol.3, 1423-1425.

Leeuwen van, W.J.D., A.R. Huete, J. Duncan, J. Franklin, 1994. Radiative transfer in shrub savanna sites in Niger -- preliminary results from HAPEX-II-Sahel: 3. Optical dynamics and vegetation index sensitivity to biomass and plant cover. Agricultural and Forest Meteorology 69, 267-288.

Leeuwen van, W.J.D., A.R. Huete., K. Didan and T. Laing, 1997a. Modeling bi-directional reflectance factors for different land cover types and surface components to standardize vegetation indices. 7th Int. Symp. Phys. Measurements and Signatures in Remote Sensing, Courcheval. (pp 1-8; in press)

Leeuwen van, W.J.D., Trevor W. Laing, and Alfredo R. Huete, 1997b. Quality Assurance of Global Vegetation Index Compositing Algorithms Using AVHRR Data. IEEE- IGARSS'97, Singapore (pp 1-3; in press)

Liou, K.N. (1980), An Introduction to Atmospheric Radiation, Academic Press, San Diego.

Liu, H.Q., and Huete, A.R., 1995, "A feedback based modification of the NDVI to minimize canopy background and atmospheric noise", IEEE Trans. Geosci. Remote Sensing, 33:457-465.

Marchuk, G.I. (1980), The Monte Carlo Methods in Atmospheric Optics, Springer-Verrlag, New York.

Mercer, R.D., Dunkelman, L., Shaw, G. E., Larson, S. M. and Kerola, D. X. (1997), Solar spectral radiance measurements: connectivity across time and place, Proceedings of the NEWRAD'97 conference, held in Tucson, Arizona, October 27-29, 1997.

Meyer, D., Verstraete, M. and Pinty, B., 1995. The effect of surface anisotropy and viewing geometry on the estimation of NDVI from AVHRR. Remote Sensing Reviews, 12:3-27.

Miura T., A. Huete, van Leeuwen. W.J.D., K. Didan, 1997. Vegetation Detection Through Smoke Filled AVIRIS images: An assessment using MODIS band passes. J. Geoph. Res.. Submitted

Moody, A. and Strahler, A.H., 1994, Characteristics of composited AVHRR data and problems in their classification. Int. J. Remote Sensing, 15(17), 3473-3491.

Myneni, R.B. and Asrar, G., 1993, Atmospheric effects and spectral vegetation indices, Remote Sens. Environ.

Myneni, R.B., Hall, F.G., Sellers, P.J., and Marshak, A.L., 1995, "The interpretation of spectral vegetation indices", IEEE Trans. Geosci. Remote Sens.

Nemani, R., Pierce, L., Running, S., and Band, L., 1993. Forest ecosystem processes at the watershed scale: sensitivity to remotely-sensed Leaf Area Index estimates. Int. J. Remote Sens. 14(13): 2519-2534.

Price, J.C., 1987. Calibration of Satellite Radiometers and the Comparison of Vegetation Indices. Rem. Sensing Environ., 21:419-422.

Prince, S.D., 1991, A model of regional primary production for use with coarse resolution satellite data. International Journal of Remote Sensing, 12(6):1313-1330.

Privette, J.L. Myneni, R.B., Emery, W.J. and Hall, F.G., 1996a. Optimal sampling conditions for estimating grassland parameters via reflectance model inversions. IEEE Trans. Geosci. Remote Sens. Vol. 34(1):272-284.

Privette, J.L., Deering, D.W., and Eck, T.E., 1996b. Estimating albedo and nadir reflectance through inversion of simple BRDF models with AVHRR/MODIS-like data. J. Geoph. Res. BOREAS special issue, submitted.

Qi, J. and Kerr, Y., 1997. On Current Compositing Algorithms. Remote Sensing Reviews, 15:235-256.

Qi, J., Huete, A.R., Hood, J., and Kerr, Y., 1994c. Compositing Multi-temporal remote sensing data sets. PECORA 11, Symposium on land information systems, Sioux Falls August 1993. p. 206-213.

Rahman, H., Pinty, B. and Verstraete, M.M., 1993. Coupled surface-atmosphere reflectance (CSAR) model 2. Semi-empirical surface model usable with NOAA AVHRR. J. Geophys. Res. 89(D11):20791-20801.

Raich, J.W., and Schlesinger, W.H., 1992, The global carbon dioxide flux in soil respiration and its relationship to vegetation and climate, Tellus 44B:81-99.

Roujean, J.L., Leroy, M., Podaire, A., and Deschamps, P.Y., 1992. Evidence of surface reflectance bidirectional effects from a NOAA/AVHRR multi-temporal data set. Int. J. Remote Sensing 13(4), 685-698.

Roy, D.P., 1997. Investigation of the maximum normalized difference Vegetation Index (NDVI) and the Maximum surface temperature (T_S) AVHRR compositing procedures for the extraction of NDVI and Ts over forest. Int. J. Remote Sens. 18(11):2383-2401.

Running, S.W., and Nemani, R.R, 1988, Relating seasonal patterns of the AVHRR vegetation index to simulated photosynthesis and transpiration of forest in different climates, Remote Sens. Environ. 24:347-367.

Running, S.W., Justice, C., Salomonson, V., Hall, D., Barker, J., Kaufmann, Y., Strahler, A., Huete, A., Muller, J.P., VanderBilt, V.,Wan, Z.M., Teillet, P. and Carneggie, D., 1994. Terrestrial Remote Sensing Science and Algorithms planned for EOS/MODIS. Int. J. Remote Sensing, Vol. 15, 17:3587-3620.

Salomonson, V.V., Barnes, W.L., Maymon, P.W., Montgomery, H.E. and Ostrow, H., 1989, MODIS: advanced facility instrument for studies of the earth as a system, IEEE Trans. Geosci. Remote Sens. 27:145-153.

Sellers, P.C. , 1985, Canopy Reflectance, photosynthesis and transpiration, Int. J. Remote Sens. 6:1335-1372

Sellers, P.J., Tucker, C.J., Collatz, G.J., Los S., Justice, C.O., Dazlich, D.A., and Randall, D.A., 1994, "A global 1° * 1° NDVI data set for climate studies. Part 2 - The adjustment of the NDVI and generation of global fields of terrestrial biophysical parameters", Int. J. Remote Sensing, 15:3519-3545.

Stowe, L.L., E.P. McClain, R. Carey, P. Pellegrino, G.G. Gutman, P. Davis, C. Long, and S. Hart. 1991. Global distribution of cloud cover derived from NOAA/AVHRR operational satellite data. Advances in Space Research, 3:51-54.

Strahler, A, et al., 1996. MODIS BRDF/Albedo Product : ATBD version 4. http://eospso.gsfc.nasa.gov/atbd/modistables. html.

Tans, P.P., Fung, I.Y., and Takahashi, T. (1990), Observational constraints on the global atmosphere CO2 budget. Science 247:1431-1438.

Teillet, P.M., Staenz, K., and Willams, D.J., 1997. Effects of Spectral, Spatial , and Radiometric Characteristics on Remote Sensing Vegetation Indices of Forested Regions. Remote Sens. Environ. 61:139-149.

Thome, K.J., Gellman, D.I., Parada, R.J., Biggar, S.F., Slater, P.N., and Moran, M.S. (1993), In-flight radiometric calibration of Landsat-5 Thematic Mapper from 1984 to present, in Proceedings of SPIE, vol. 1938, 126-130.

Tomasko, M.G. and Doose, L.R. (1989), private communication.

Townshend, J.R.G., 1994, Global data sets for land applications from the AVHRR: an introduction. Int. J. Remote Sensing, 15:3319-3332.

Townshend, J.R.G., C. Justice, W. Li, C. Gurney, and J. McManus, 1991, "Global land cover classification by remote sensing: present capabilities and future possibilities", Remote Sens. Environ., 35:243-256.

Townshend, J.R.G., Justice, C.O., Gurney, C. and McManus, J., 1992, The impact of misregistration on the detection of changes in land cover, IEEE Trans. Geosci. Remote Sens., 30(5):1054-1060.

Tucker, C.J. and Sellers, P.J., 1986, Satellite remote sensing of primary productivity, International Journal of Remote Sensing, 7:1395-1416.

Vermote, E., Remer, L.A., Justice, C.O., Kaufman, Y.J., and Tanré, 1995, ATBD Atmosphere correction algorithm: Spectral reflectances (MOD09), Version 2.

Vermote, E., Tanré, D., Deuzé, J.L., Herman, M., and Mocrette, J.J., 1997, Second Simulation of the Satellite Signal in the Solar Spectrum: an overview. IEEE Trans. Geosc. Remote Sens., 35(3):675-686.

Vermote, E.F., Tanre, D., Deuze, J.L., Herman, M. and Morcrette, JJ. (1997), Second simulation of the satellite signal in the solar spectrum, 6S: an overview, IEEE Transactions on Geoscience and Remote Sensing, 35, No. 3, 675-686.

Vierling, L.A., Deering, D.W., Eck, T.F., 1997. Differences in Arctic Tundra Vegetation Type and Phenology as Seen Using Bidirectional Radiometry in the Early Growing Season. Remote Sens. Environ. 60:71-82.

Viovy, N., Arino, O. and Belward, A.S., 1992. The best index slope extraction (BISE): A method for reducing noise in NDVI time series. Int. J. Rem. Sensing, Vol:13, 8:1585-1590.

Walter-Shea, E.A., Privette, J., Cornell, D., Mesarch, M.A., Hays, C.J., 1997, Relationship between directional spectral vegetation indices and leaf area and absorbed radiation in alfalfa. Remote Sens. Environ. (In press)

Walthall, C.L., Norman, J.M., Welles, J.M., Campbell, G., and Blad, B.L., 1985, Simple equation to approximate the bi-directional reflectance from vegetative canopies and bare soil surfaces," Applied Optics, 24(3), pp. 383-387.

Wanner W., A.H. Strahler, B. Hu, P. Lewis, J.-P. Muller, X.. Li, C.L. Barker Schaaf, and M.J. Barnsley, 1997. Global retrieval of bidirectional reflectance and albedo over land from EOS MODIS and MISR data: Theory and algorithm. J. Geoph. Res., 102, D14, 17143-17161.

Wanner W., X.. Li, A.H. Strahler, 1995. On the Derivation of kernel-driven models of bidirectional reflectance. J. Geoph. Res., 100, D10, 21077-21089

Wolfe. R., D. Roy. Georegistration of MODIS data (level 2G), to be submitted

Wu, A., Li, Z. and Cihlar, 1995, Effects of land cover type and greenness on advanced very high resolution radiometer bidirectional reflectances: Analysis and removal. J. Geophys. Res., 100(D5), 9179-9192.